

Lattice effect on the superexchange interaction in antiferromagnetic $\text{Bi}_2\text{Sr}_2\text{CaCu}_2\text{O}_8$

Jie Xin,^{1,2} Alexander G. Gavriliuk,^{3,4,5} Jia-Wei Hu,² Jian-Bo Zhang,² Gen-Da Gu,⁶ Viktor V. Struzhkin,² Alexander F. Goncharov,⁷ Hai-Qing Lin,⁸ Ho-Kwang Mao,² and Xiao-Jia Chen^{2,9,*}

¹*Department of Physics and State Key Laboratory of Surface Physics, Fudan University, Shanghai 200438, China*

²*Center for High Pressure Science and Technology Advanced Research, Shanghai 201203, China*

³*Institute for Nuclear Research, Russian Academy of Sciences, Moscow, Troitsk 108840, Russia*

⁴*FSRC Crystallography and Photonics of Russian Academy of Sciences, Moscow 119333, Russia*

⁵*REC Functional Nanomaterials, Immanuel Kant Baltic Federal University, Kaliningrad 236041, Russia*

⁶*Condensed Matter Physics and Materials Science,*

Brookhaven National Laboratory, New York 11973, USA

⁷*Earth and Planets Laboratory, Carnegie Institution for Science, Washington, DC 20015, USA*

⁸*School of Physics, Zhejiang University, Hangzhou 310058, China*

⁹*School of Science, Harbin Institute of Technology, Shenzhen 518055, China*

(Dated: April 25, 2023)

The in-plane superexchange interaction J of cuprate superconductors has long been suggested to be an important parameter for exploring their high-temperature superconductivity. The bilayer $\text{Bi}_2\text{Sr}_2\text{CaCu}_2\text{O}_{8+\delta}$ is the most studied system with high-quality single crystals in the wide doping range with the same structure and phase. So far, the lattice parameter dependence of J in its antiferromagnetic parent compound $\text{Bi}_2\text{Sr}_2\text{CaCu}_2\text{O}_8$ has not been established. By combining Raman scattering and x-ray diffraction techniques on the same sample in the same pressure environment, we obtain the evolution of both the two-magnon spectrum and the structural parameters with pressure up to nearly 30 GPa. The relationship between pressure or the in-plane lattice parameter and J is thus established for $\text{Bi}_2\text{Sr}_2\text{CaCu}_2\text{O}_8$. Over the studied pressure range, superconductivity does not appear in this parent compound based on a sensitive magnetic measurement technique. The effects of pressure and chemical doping on the superexchange interaction and structure and their implications for superconductivity are discussed from the comparison of the obtained experimental data with the existing experiments. The results and findings provide valuable information for the understanding of superconductivity and the future theory developments for superconductivity in cuprates.

I. INTRODUCTION

Since the high-temperature superconductivity was discovered in cuprates^{1,2}, extensive experimental and theoretical researches have been carried out with many important findings. However, a comprehensive theoretical understanding of superconductivity in cuprates remains elusive. Resonating valence bonds^{3,4} and spin-fluctuation mediated^{5,6} scenarios are among the most promising theoretical approaches in describing superconductivity in cuprates. In such spin-related theories, the Cu-O-Cu superexchange interaction, denoted by J , is considered to be the cause of pairing. In the spin-fluctuation mediated scenario, electrons are paired up by exchanging magnetic spin fluctuations, which are also governed by J ⁶. The J value can be determined conveniently from the two-magnon spectrum based on Raman scattering spectroscopy⁷. The quantitative determination of J has been given for antiferromagnetic La_2CuO_4 ⁸⁻¹⁰ and $\text{YBa}_2\text{Cu}_3\text{O}_6$ ¹¹ based on the Raman scattering spectroscopy after the discoveries of superconductivity in these two families. Extensive experiments further revealed that J changes with doping in a similar manner as the pseudogap and pair peak in almost all cuprate superconductors^{9,11-15}. These similarities indicate that the high-energy magnetic fluctuations are possibly indeed involved in the formation of the pseudo-

gap and the Cooper pairing. Such an evolution from the high-energy excitation to superconducting quasiparticles has been suggested from coherent charge fluctuation spectroscopy¹⁶. The development from the two-magnon peak to a quasiparticle response with doping has been reproduced theoretically¹⁷. Interestingly, there is a report for the existence of an approximately linear relationship between J and the maximum critical temperature T_c for many optimally doped cuprates¹⁸. These results seemingly indicate the significance of J and its connection to the superconductivity in cuprates. While emphasizing the importance of this parameter for the understanding of superconductivity, one will need to have the quantitative relationship between the lattice parameter and J . However, such information is rare¹⁹ and difficult to be drawn from the existing experiments of many superconducting families^{8-15,18}.

Applying pressure has been proven to provide a clean and effective tool to tune the structural, magnetic, and superconducting properties²⁰. Raman spectra of many materials including cuprates can be collected at high pressures²¹. The high-pressure two-magnon spectra of the parent compounds²²⁻²⁵ of two important cuprate families have been obtained by using Raman spectroscopy. High-pressure J behaviors were thus established for La_2CuO_4 ²², Eu_2CuO_4 ^{23,25}, $\text{Sr}_2\text{CuCl}_2\text{O}_2$ ²⁴, and $\text{YBa}_2\text{Cu}_3\text{O}_{6.2}$ ²⁵. To simplify the traditionally complicated theoretical expression for J , the lattice parameter

dependence of J is expressed by a power law, $J \sim d^{-n}$, where d is the in-plane Cu-O-Cu bonding length and n is an empirically determined constant. In order to establish the accurate relationship between d and J , one needs to determine the structural evolution with pressure for the studied material at the same environments of composition, temperature, and pressure etc. Based on the structural information in the literature, the estimated relationships have been given for La_2CuO_4 with $J \sim d^{-(6.4 \pm 0.8)}$ ²², Eu_2CuO_4 and $\text{YBa}_2\text{Cu}_3\text{O}_{6.2}$ with $J \sim d^{-(3.0 \pm 0.5)}$ ²⁵. Here the empirical constant n does not differ too much with the one appeared in $J \sim d^{-(4 \pm 2)}$ for M_2CuO_4 ($\text{M}=\text{Pr}, \text{Nd}, \text{Sm}, \text{Eu}, \text{and Gd}$)¹⁹. The well designed experiments on an insulating compound $\text{Bi}_{1.98}\text{Sr}_{2.06}\text{Y}_{0.68}\text{CaCu}_2\text{O}_{8.03}$ with neon as pressure transmitting medium gave $J \sim d^{-10.33}$ ²⁶. It remains unknown whether the large n value is due to the lattice distortion or internal pressure induced by Y substitution for Ca in the studied system²⁷. So far, such an accurate relationship for an antiferromagnetic parent cuprate has not been established yet based on the simultaneous spectroscopy and diffraction measurements on the same sample in the same pressure environments. This is obviously an urgent subject in order to elucidate the spin-related pairing mechanism for superconductivity in high- T_c cuprates.

This work is designed to solve the above mentioned problem with the help of high-quality single crystals of $\text{Bi}_2\text{Sr}_2\text{CaCu}_2\text{O}_{8+\delta}$. The composition choice of the samples hopes to eliminate the possible external effect resulting from the elemental substitution and draw the information solely due to the application of pressure. After characterizing the antiferromagnetic feature of the chosen single crystal $\text{Bi}_2\text{Sr}_2\text{CaCu}_2\text{O}_8$ (with the doping level $\delta \sim 0$), we perform high-pressure measurements of Raman scattering and x-ray diffraction (XRD) to obtain the spectroscopic and structural properties at high pressures. The evolution of the two-magnon spectrum with pressure for $\text{Bi}_2\text{Sr}_2\text{CaCu}_2\text{O}_8$ is obtained after the comparison of the spectroscopic character of a nearly optimally doped $\text{Bi}_2\text{Sr}_2\text{CaCu}_2\text{O}_{8+\delta}$ loaded together in the sample chamber near $\text{Bi}_2\text{Sr}_2\text{CaCu}_2\text{O}_8$. The pressure (or lattice parameter) dependence of J is determined for $\text{Bi}_2\text{Sr}_2\text{CaCu}_2\text{O}_8$. Within the studied pressure regime and same pressure environment, the idea of pressure-induced superconductivity in $\text{Bi}_2\text{Sr}_2\text{CaCu}_2\text{O}_8$ is experimentally examined based on a highly sensitive magnetic detection technique. We also discuss the possible factors controlling superconductivity from the comparisons of the present and available experiments.

II. EXPERIMENTAL DETAILS

The single crystals of $\text{Bi}_2\text{Sr}_2\text{CaCu}_2\text{O}_{8+\delta}$ grown using the floating zone technique were detailed previously²⁸. Magnetization measurements were used to characterize the magnetic feature and superconducting transition of the synthesized samples by combining a supercon-

ducting quantum interference device magnetometer (Quantum Design MPMS3) and an in-house highly sensitive magnetic detection instrument. The latter was developed for detecting superconductivity for the sample with small dimensions in diamond anvil cell (DAC) at high pressures^{20,29,30}. This technique is based on the suppression of the Meissner effect and quenching of superconductivity in the sample by an external magnetic field. The magnetic field applied to the sample inserted in the DAC mainly affects the signal coming from the sample. If the sample is superconducting, its transition temperature can be identified at the point where the signal goes to zero due to the disappearance of the Meissner effect. This highly sensitive technique has been used to discover superconductivity in compressed sulfur³¹ and lithium³² and study the pressure effect on T_c in conventional superconductor NbN ³³ and various cuprates including $\text{YBa}_2\text{Cu}_3\text{O}_{7-\delta}$ ³⁴, $\text{Bi}_2\text{Sr}_2\text{Ca}_{n-1}\text{Cu}_n\text{O}_{2n+4+\delta}$ ($n=2,3$)^{30,35}, $\text{Tl}_2\text{Ba}_2\text{CaCu}_2\text{O}_{8+\delta}$ ³⁶, and $\text{HgBa}_2\text{CuO}_{4+\delta}$ ³⁷.

In the current study, we loaded nearly optimally doped $\text{Bi}_2\text{Sr}_2\text{CaCu}_2\text{O}_{8+\delta}$ crystal as a reference and an antiferromagnetic $\text{Bi}_2\text{Sr}_2\text{CaCu}_2\text{O}_8$ crystal separately into a DAC. The crystal was cut in the dimensions of approximately $100 \times 100 \times 20 \mu\text{m}^3$. It was loaded with a ruby chip together into a sample chamber in a gasket made by non-magnetic Ni-Cr alloy. The gasket is pressed in between two diamond anvils with diameter of $300 \mu\text{m}$ in a DAC made by nonmagnetic Be-Cu alloy. The layout of such instruments and designs were given in detail previously^{20,29,30}. The DAC was then mounted in a low-temperature cryostat with accessible optical windows, manufactured from Cryo Industries of America, Inc. The pressure can be mechanically tuned at demanded pressure and temperature. In such a design, Raman spectrum of the sample in DAC can be collected at the desired temperature and pressure. The temperature was monitored from the silicon diode sensor attached to the DAC in close proximity to the sample with a typical precision of $\pm 0.5 \text{ K}$. The pressure level was gauged based the shift of the $R1$ fluorescence line of ruby³⁸ with the correction of temperature effect. For high-pressure magnetic susceptibility measurements, we changed and measured pressure at temperature of about 120 K . Below this temperature, the pressure can maintain a nearly constant value at low temperatures for the DAC and gasket in such an instrument.

To have the consistency of the spectroscopy and structure data for the comparison, we conducted the measurements of high-pressure Raman scattering and XRD measurements on $\text{Bi}_2\text{Sr}_2\text{CaCu}_2\text{O}_8$ at room temperature. In fact, the spectroscopic signature of the two-magnon scattering for our studied $\text{Bi}_2\text{Sr}_2\text{CaCu}_2\text{O}_8$ is not strong. For comparison, we loaded this crystal together with a nearly optimally doped crystal nearby into a sample chamber (about $120 \mu\text{m}$ in diameter and $30 \mu\text{m}$ in thickness) of a DAC with a pair of diamond anvils in diameter of $300 \mu\text{m}$. Both crystals were freshly cleaved with shin-

ing surfaces. A chip of ruby was put near the edge of the chamber filled with neon as the pressure medium. The Raman scattering signal was created by the Coherent sapphire laser device with 488 nm wavelength to illuminate an approximate $5 \times 5 \mu\text{m}^2$ spot on the crystal surface. The low 2 mW power of the laser was chosen in order to avoid the over-heating of the sample. Raman spectra were collected in the back-scattering geometry. For each pressure of interest, we collected the Raman spectra of the two crystals one by one by keeping the same measurement conditions such as collecting time and laser grating. The Raman spectrum of the nearly optimally doped $\text{Bi}_2\text{Sr}_2\text{CaCu}_2\text{O}_{8+\delta}$ at each studied pressure exhibits a nearly flat background in the two-magnon scattering wavenumber range. The weak two-magnon scattering spectrum of $\text{Bi}_2\text{Sr}_2\text{CaCu}_2\text{O}_8$ at the same pressure can be picked up and enlarged by subtracting the nearly flat background from the nearly optimally doped $\text{Bi}_2\text{Sr}_2\text{CaCu}_2\text{O}_{8+\delta}$.

Synchrotron XRD experiments were conducted at the 16BM-D beamline of the High Pressure Collaborative Access Team (HPCAT) at the Advanced Photon Source (APS) of Argonne National Laboratory, with an incident x-ray wavelength of 0.424603 Å. $\text{Bi}_2\text{Sr}_2\text{CaCu}_2\text{O}_8$ crystal was finely ground into powders to obtain good diffraction data. The powders were pressed into a small piece. It was then loaded into a symmetric DAC with anvils in diameter of 300 μm together with a small ruby chip to monitor the pressure. Neon was used as the pressure-transmitting medium. The diffraction patterns were collected at room temperature at pressures up to 34 GPa. The two-dimensional patterns were integrated into 2θ vs. intensity data using Fit2D software³⁹. The diffraction patterns were analyzed using the Le Bail method in terms of the GSAS-II package⁴⁰.

It should be mentioned that in all these measurements, the samples were kept in the neon environment. The experimental data for $\text{Bi}_2\text{Sr}_2\text{CaCu}_2\text{O}_8$ were collected and analyzed on the same single crystal. These considerations are expected to provide the consistent and reliable data of the studied system.

III. RESULTS AND DISCUSSION

A. Sample characterization

The characterization of the quantum ground state of $\text{Bi}_2\text{Sr}_2\text{CaCu}_2\text{O}_8$ is given from the magnetization measurements (Fig. 1). There is an antiferromagnetic-paramagnetic transition at the Néel temperature (T_N) of 90 K, indicated by the kink in the temperature dependence of the magnetic moment in a magnetic field directed along the c axis. No evidence for supporting superconductivity is provided from the magnetic susceptibility data down to 2 K. The kink for the antiferromagnetic transition in studied $\text{Bi}_2\text{Sr}_2\text{CaCu}_2\text{O}_8$ is similar to those found in other antiferromagnetic cuprates

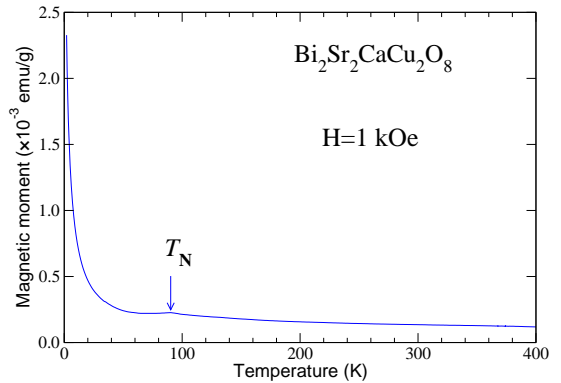


FIG. 1. Temperature dependence of the magnetic susceptibility of $\text{Bi}_2\text{Sr}_2\text{CaCu}_2\text{O}_8$ measured with a magnetic field of 1 kOe at ambient pressure.

such as $\text{Bi}_2\text{Sr}_2\text{Ca}_{1-x}\text{Y}_x\text{Cu}_2\text{O}_{8+\delta}$ ⁴¹, $\text{La}_2\text{CuO}_{4+\delta}$ ⁴² and $\text{Bi}_2\text{SrLaCuO}_y$ ⁴³. No magnetic phase transition has ever been reported for $\text{Bi}_2\text{Sr}_2\text{CaCu}_2\text{O}_{8+\delta}$ ⁴³. The T_N value obtained for the studied $\text{Bi}_2\text{Sr}_2\text{CaCu}_2\text{O}_8$ compound is 20 K higher than those in the $\text{Bi}_2\text{Sr}_2\text{Ca}_{1-x}\text{Y}_x\text{Cu}_2\text{O}_{8+\delta}$ system⁴¹. This result indicates the good antiferromagnetic character of our sample. Its relatively high T_N value also corresponds to the extremely low content of excess oxygen. Thus, the content of excess oxygen in the studied sample is assumed to be zero (that is, $\delta \sim 0$). Therefore, we have a sample in the normal composition of $\text{Bi}_2\text{Sr}_2\text{CaCu}_2\text{O}_8$ with the antiferromagnetic nature for further investigations.

B. Two-magnon scattering at high pressures

Antiferromagnetism is the striking physical feature of the parent cuprates. A classical spin-wave is acoustic-like, which means that a magnon (single-spin flip) excitation can hardly be observed in the inelastic light scattering channel. However, two neighboring spins on Cu sites bridged by intermediate oxygen ions may reverse their spin directions simultaneously. This process meets the requirements of selection rules for the so-called two-magnon process permitted in Raman scattering. The double spin-flop excitations (two-magnon) on CuO_2 layers could be directly probed by the Raman scattering technique. As the simultaneous reversal of two adjacent spins costs the energy of the nearest six superexchange coupling constants, the two-magnon peak should appear at about $3J$ in energy. Due to the magnon-magnon interaction, the ratio slightly deviates from 3, and this ratio is taken as 2.7 based on the two-dimensional Heisenberg model⁴⁴.

For a parent cuprate, previous Raman scattering studies detected the two-magnon peak around 3000 cm^{-1} at ambient pressure, corresponding to a J of $\sim 1000 \text{ cm}^{-1}$ (about 125 meV)⁸⁻¹¹. This spectrum range just overlaps with the two-phonon Raman peak of the diamond

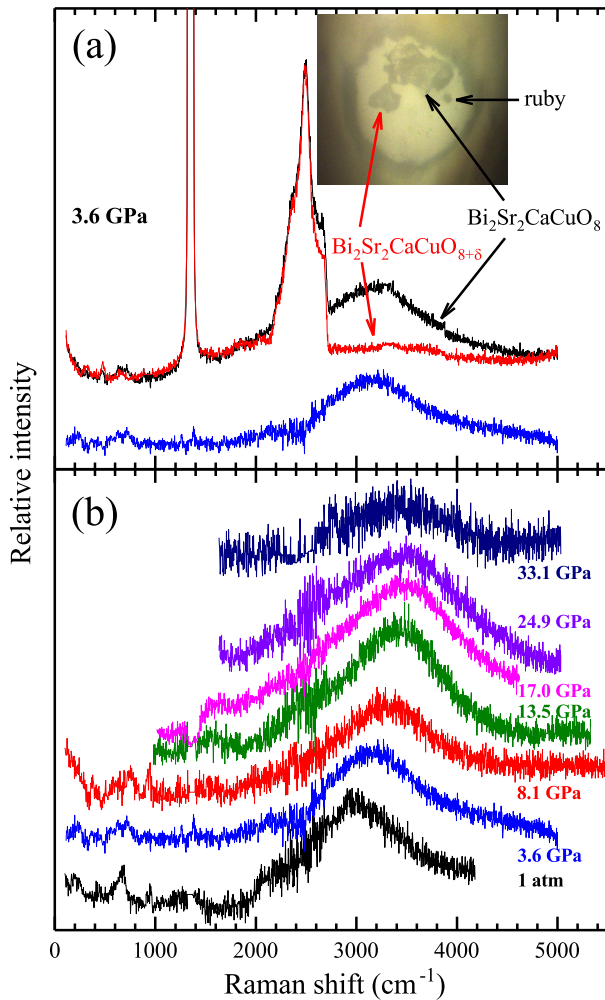


FIG. 2. Two-magnon Raman scattering spectra for antiferromagnetic $\text{Bi}_2\text{Sr}_2\text{CaCu}_2\text{O}_8$ under pressure. (a) Raman spectra of the antiferromagnetic (black curve) and nearly optimally doped (red curve) $\text{Bi}_2\text{Sr}_2\text{CaCu}_2\text{O}_{8+\delta}$ at pressure of 3.6 GPa. The blue curve corresponds to the spectrum subtraction from the signal of the antiferromagnetic sample to that of the nearly optimally doped one. Inset: Photograph of two crystals in neon environment with a ruby chip. (b) Subtracted two-magnon scattering spectra of $\text{Bi}_2\text{Sr}_2\text{CaCu}_2\text{O}_8$ at representative pressures in the compression run.

(around 2500 cm^{-1}). Therefore, the collection of the two-magnon spectrum is a challenge by using diamond anvils. This is probably a reason why the high-pressure behaviors of the two-magnon Raman scattering for many parent cuprates have not been reached yet. To solve this critical problem, we loaded the antiferromagnetic $\text{Bi}_2\text{Sr}_2\text{CaCu}_2\text{O}_8$ crystal together with a nearly optimally doped $\text{Bi}_2\text{Sr}_2\text{CaCu}_2\text{O}_{8+\delta}$ into a DAC (Inset of Fig. 2(a)). By performing the measurements at the same conditions, we obtained the Raman spectra of them. As an example, the Raman spectra at 3.6 GPa are shown in Fig. 2(a). With the assumption of the same active Raman feature from the used diamond anvils or medium for the

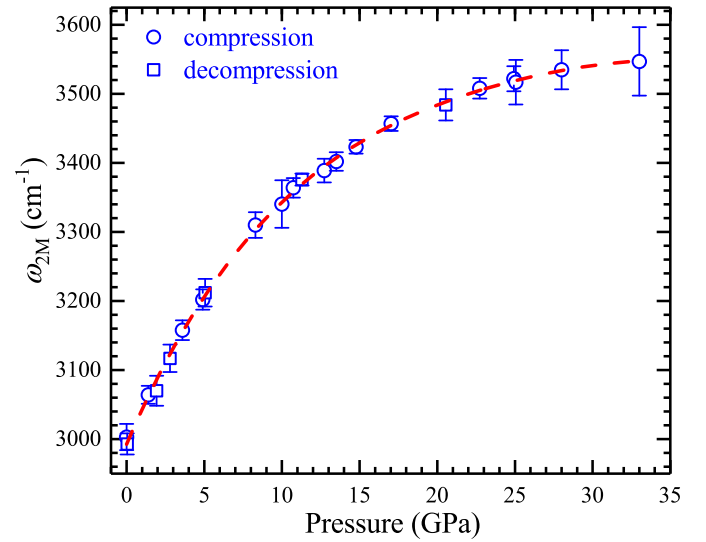


FIG. 3. Pressure dependence of the two-magnon frequency in antiferromagnetic $\text{Bi}_2\text{Sr}_2\text{CaCu}_2\text{O}_8$ in the compression and decompression run. The dashed curve is the polynomial fitting to the data points for the guide to the eyes.

studied two crystals at the measured pressure, the strong two-magnon scattering spectrum of $\text{Bi}_2\text{Sr}_2\text{CaCu}_2\text{O}_8$ can be derived by subtracting the collected spectrum from that of $\text{Bi}_2\text{Sr}_2\text{CaCu}_2\text{O}_{8+\delta}$. This procedure turned out to be very successful. As can be seen, the two-magnon frequency of $\text{Bi}_2\text{Sr}_2\text{CaCu}_2\text{O}_8$ at ambient pressure is well situated in the trend of $\text{Bi}_2\text{Sr}_2\text{CaCu}_2\text{O}_{8+\delta}$ with the different dopants^{12,13}. The positions of the phonon modes at the low wavenumbers are also consistent with those reported from Raman measurements^{45,46}.

Figure 2(b) shows the two-magnon Raman scattering spectra of $\text{Bi}_2\text{Sr}_2\text{CaCu}_2\text{O}_8$ at various pressures up to 33.1 GPa. The two-magnon scattering signal was recorded during the compression and decompression run. As pressure is increased, the two-magnon peak broadens and shifts to higher wavenumbers (or energies) with the decrease of the intensity. These behaviors are consistent with the early reports for La_2CuO_4 up to 10 GPa²², Eu_2CuO_4 up to 41 GPa²⁵, $\text{YBa}_2\text{Cu}_3\text{O}_{6.2}$ up to 43 GPa²⁵, and $\text{Bi}_{1.98}\text{Sr}_{2.06}\text{Y}_{0.68}\text{CaCu}_2\text{O}_{8.03}$ up to 32 GPa²⁶. The evolution of the two-magnon frequency (ω_{2M}) with pressure for $\text{Bi}_2\text{Sr}_2\text{CaCu}_2\text{O}_8$ is given in Fig. 3. As can be seen, ω_{2M} increases continuously from nearly 3000 to 3550 cm^{-1} with increasing pressure within the studied pressure range, as observed previously for La_2CuO_4 ²², $\text{Sr}_2\text{CuCl}_2\text{O}_2$ ²⁴, and $\text{Bi}_{1.98}\text{Sr}_{2.06}\text{Y}_{0.68}\text{CaCu}_2\text{O}_{8.03}$ ²⁶. It is interesting to notice the nearly linear change of ω_{2M} with pressure were observed in the early studies on Eu_2CuO_4 ²⁵ and $\text{YBa}_2\text{Cu}_3\text{O}_{6.2}$ ²⁵ over the studied pressure range. The increase of ω_{2M} for $\text{Bi}_2\text{Sr}_2\text{CaCu}_2\text{O}_8$ upon the applied pressure to 33 GPa is almost the same as La_2CuO_4 ²² within 10 GPa. However, $\text{Bi}_{1.98}\text{Sr}_{2.06}\text{Y}_{0.68}\text{CaCu}_2\text{O}_{8.03}$ ²⁶ exhibits a large increase of ω_{2M} from the nearly same initial value to above 4000 cm^{-1} within the nearly same

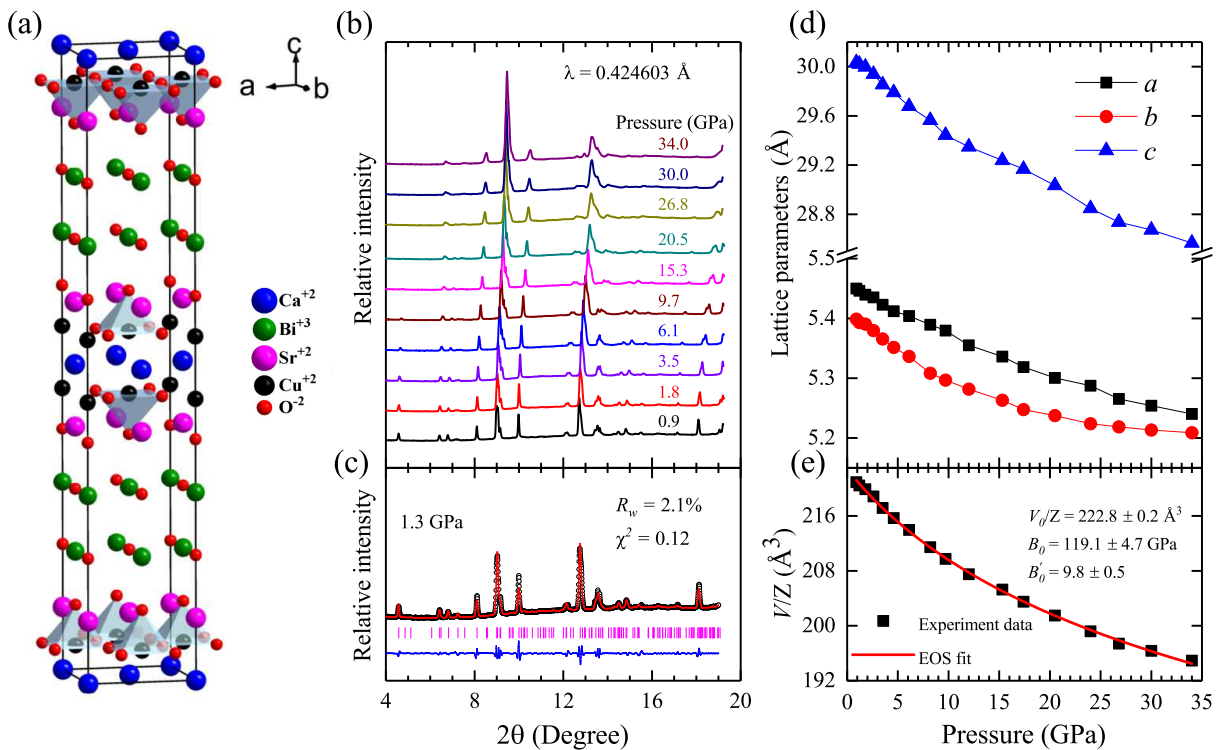


FIG. 4. Structural properties of antiferromagnetic $\text{Bi}_2\text{Sr}_2\text{CaCu}_2\text{O}_8$ at high pressures. (a) The schematic orthorhombic structure with the space group of $Amaa$. (b) The integrated x-ray diffraction data at representative pressures. (c) The observed XRD patterns (circles), Le Bail fitting (red line), and their difference (blue line) between the observed and calculated profiles at pressure of 1.3 GPa. The vertical bars refer to the peak positions. (d) The lattice parameters along the a , b , and c axis as a function of pressure. (e) Pressure dependence of the unit-cell volume V/Z .

pressure range as the present study. In all these measurements on cuprates, an increasing ω_{2M} upon lattice compression is generic. This can be considered as the common feature of ω_{2M} for cuprates at high pressures.

Superconductivity in cuprates was found to develop with the suppression of the antiferromagnetic order upon doping. It has been generally believed that the application of pressure has the equivalent effect on superconductivity as the chemical doping in these compounds. For comparison, the two-magnon peak behaves with doping in an opposite way as pressure. Upon doping, the two-magnon peak indeed becomes broader but moves to lower wavenumber^{9,11–15,47,48}. The totally different change directions for the two-magnon frequency from doping and pressure suggest their different effects if the superexchange interaction is tightly related to superconductivity.

C. Structural evolution with pressure

To obtain the evolution of ω_{2M} (thus J) against the lattice parameters, we conducted synchrotron XRD measurements for $\text{Bi}_2\text{Sr}_2\text{CaCu}_2\text{O}_8$ at various pressures up to 34 GPa. The schematic crystal structure of this material, belonging to the space group of $Amaa$ ⁴⁹, is shown in Fig. 4(a). This structure consists of two equivalent

perovskite sub-cells with respect to each other along the diagonal direction in the giving a - b plane and bonded by Van der Waals force. Each sub-cell consists of two insulating BiO layers and two SrO layers. In the middle of the sub-cell, two structurally equivalent CuO_2 layers are separated by the Ca layer. These layers are stacked in the sequence of $\text{BiO-SrO-CuO}_2\text{-Ca-CuO}_2\text{-SrO-BiO}$.

The powder XRD results of $\text{Bi}_2\text{Sr}_2\text{CaCu}_2\text{O}_8$ at high pressures and room temperature are presented in Fig. 4(b). With the application of pressure, all diffraction peaks gradually shift to high angles, indicating the lattice shrinking. No new diffraction peaks appear. There is also no peak merging or splitting. These observations indicate no structural transformation under pressure. The compound maintains the same structure at the studied pressure range, consistent with previous high-pressure structural studies on this system^{50,51}.

Different from other cuprate families, Bi-based system possesses an incommensurate structure modulation along the b axis^{52–55}. The evolution of the modulation vector for bilayer $\text{Bi}_2\text{Sr}_2\text{CaCu}_2\text{O}_{8+\delta}$ with pressure has never been reported. We observed a weak but regular peak in low angle of about 1° at each applied pressure (not shown in Fig. 4(b)), consistent with the early observations^{54,55}. This peak is considered the first-order diffraction peak from the modulation superstructure. The component of

modulation vector \vec{b}^* can be calculated from this peak position. The vector component b^* is found to be around 0.22 and remains unchanged within the studied pressure range.

The refinement of the crystal structure of $\text{Bi}_2\text{Sr}_2\text{CaCu}_2\text{O}_8$ is not an easy task. We believe that the lattice parameters can be determined by Le Bail fitting to the average structure model with sufficient accuracy. Figure 4(c) illustrates the powder XRD data and Le Bail fitting for $\text{Bi}_2\text{Sr}_2\text{CaCu}_2\text{O}_8$ at pressure of 1.3 GPa based on the structure model depicted in Fig. 4(a). The fitting provides reasonable factors of $R_w = 2.1\%$ and $\chi^2 = 0.12$. The similar fittings to the collected diffraction patterns provide the lattice parameters with comparable quality up to 34 GPa. These results indicate that $\text{Bi}_2\text{Sr}_2\text{CaCu}_2\text{O}_8$ keeps in an orthorhombic structure within the studied pressure range. Figure 4(d) shows the pressure dependence of the lattice parameters along the a , b , and c axis. The corresponding unit-cell volume V with Z of 4 being the number of the chemical formula per unit cell is presented in Fig. 4(e). The lattice parameters and cell volume decrease gradually with the increase of pressure. The pressure-volume data are fitted using the third-order Birch-Murnaghan equation of states (EOS)⁵⁶, as shown by the curve in Fig. 4(e). The fitting gives the bulk modulus at zero pressure $B_0 = 119.1 \pm 4.7$ GPa, the initial unit cell volume per chemical formula $V_0/Z = 222.8 \pm 0.2 \text{ \AA}^3$ and the first pressure derivative of the bulk modulus at zero pressure $B'_0 = 9.8 \pm 0.5$ for $\text{Bi}_2\text{Sr}_2\text{CaCu}_2\text{O}_8$. The obtained B_0 value is bigger than the one reported for underdoped $\text{Bi}_2\text{Sr}_2\text{CaCu}_2\text{O}_{8+\delta}$ with $B_0 = 114.9 \pm 6.4$ GPa⁵¹, and much larger than the reported value of 73 GPa⁵⁷, 62.5 GPa⁵⁰, and 68.6 GPa⁵⁸ for Bi-based compounds. The dramatic difference in B_0 comes from the difference in samples and the experimental conditions.

The change of the obtained lattice parameters of antiferromagnetic $\text{Bi}_2\text{Sr}_2\text{CaCu}_2\text{O}_8$ under pressure is again used to compare the doping effect on the crystal structure. Amongst all discovered cuprate superconductors, bilayer $\text{Bi}_2\text{Sr}_2\text{CaCu}_2\text{O}_{8+\delta}$ is a most studied superconducting system with the complete phase diagram^{59,60} over the whole doping range covering from the slightly underdoped region through the optimal level to the heavily overdoped regime. Interestingly, the structural properties of this system as a function of oxygen content over the whole doping range have not fully been investigated yet. To date, no systematic evolution of the lattice parameter(s) with doping is available for $\text{Bi}_2\text{Sr}_2\text{CaCu}_2\text{O}_{8+\delta}$ over a relatively wide doping range^{61,62}, probably due to the complexity in the structure determination^{52–55}. The annealing of as-grown samples with increasing partial oxygen pressure leads to the increase of the oxygen content. At such conditions, T_c was reported to decrease with oxygen pressure in a similar way as the reduction of the c -axis lattice constant⁶¹. This observation seemingly indicates the c -axis lattice parameter decreases in the overdoped regime. On the other hand, the similar

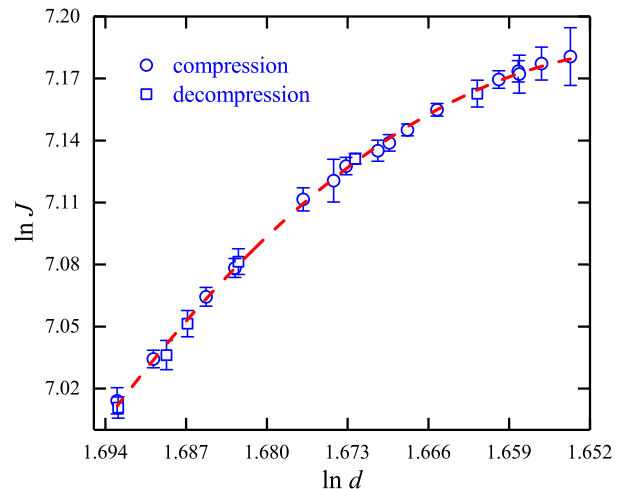


FIG. 5. The double logarithmic plot of in-plane J versus the average in-plane lattice parameter d . The dashed curve is the fitting to the data points.

trend for the c -axis lattice parameter was found with the loss of oxygen for the single-phase $\text{Bi}_2\text{Sr}_2\text{CaCu}_2\text{O}_{8+\delta}$ ⁶². Since the annealing of the as-grown crystal simulates the underdoping effect, this behavior suggests the reduction of the c -axis lattice parameter in the underdoped regime. Although the exact c values do not match each other even for their different as-grown samples, these two sets of experiments^{61,62} indicate the continuous decrease of the c -axis lattice parameter upon the carrier concentration. There are not any clear trends for the lattice parameters along the a and b direction from these experiments^{61,62}. The observed reduction of the c lattice parameter for $\text{Bi}_2\text{Sr}_2\text{CaCu}_2\text{O}_8$ may imply the increase of the carrier concentration by the application of pressure.

D. Relation between the in-plane superexchange interaction J and the lattice parameter

Having determined the pressure dependence of ω_{2M} and the equation of states for $\text{Bi}_2\text{Sr}_2\text{CaCu}_2\text{O}_8$, we can obtain the lattice parameter dependence of ω_{2M} after converting the pressure into the lattice parameter. Such a dependence for the in-plane superexchange interaction J can be directly obtained through the expression $\omega_{2M} = 2.7J^{44}$. For layered cuprates, the in-plane superexchange interaction J is insensitive to the out-of-plane coupling. One can only consider the parameters within the CuO_2 plane. There is a slight difference between the lattice parameters along the a and b axis for $\text{Bi}_2\text{Sr}_2\text{CaCu}_2\text{O}_8$. It is reasonable to define the average lattice constant in the a - b plane as $d = \sqrt{ab}$. The d value at the given pressure for the corresponding ω_{2M} (or J) is thus obtained from the determined equation of states based on the expression of $V/Z = d^2c/4$.

To determine the exponent n in $J \sim d^{-n}$ for

$\text{Bi}_2\text{Sr}_2\text{CaCu}_2\text{O}_8$, we plotted $\ln J$ as a function of $\ln d$ in Fig. 5. We observed a linear dependence of $\ln J$ on $\ln d$ within 6 GPa. By performing a linear fitting of the $\ln J - \ln d$ data in this pressure range, we obtained the relationship of $J \sim d^{-(6.6 \pm 0.2)}$. At high pressures (> 6 GPa), the dependence of $\ln J$ on $\ln d$ gradually deviates downwards from linear behavior, and the deviation increases with pressure. This indicates that the exponent n in the empirical formula $J \sim d^{-n}$ decreases with increasing pressure, implying reduced sensitivity of J to d at higher pressures as observed in La_2CuO_4 ²².

Compared with other cuprates, the lattice parameter dependence of J in $\text{Bi}_2\text{Sr}_2\text{CaCu}_2\text{O}_8$ is close to those of La_2CuO_4 ($J \sim d^{-(6.4 \pm 0.8)}$)²², Eu_2CuO_4 and $\text{YBa}_2\text{Cu}_3\text{O}_{6.2}$ ($J \sim d^{-(3.0 \pm 0.5)}$)²⁵, and M_2CuO_4 ($\text{M} = \text{Pr}, \text{Nd}, \text{Sm}, \text{Eu}$ and Gd) ($J \sim d^{-(4 \pm 2)}$)¹⁹, but differs substantially from that of $\text{Bi}_{1.98}\text{Sr}_{2.06}\text{Y}_{0.68}\text{CaCu}_2\text{O}_{8+\delta}$ ($J \sim d^{-10.33}$)²⁶. Considering the fact that this relationship is established based on the simultaneous Raman and XRD measurements on the same characterized crystal at the nearly equal experimental conditions, we hope it to shed light on important features for the establishment and understanding of the mechanism of superconductivity in high- T_c cuprates.

E. Examination of possible superconductivity under pressure

It has been generally believed that superconductivity can be created by doping or pressure in high- T_c cuprates. This belief has been proven from the similar phase diagram of T_c with these two tuning modes in strongly correlated superconductors such as heavy fermions^{63–65} or iron-based compounds^{66–68}. In those superconductors, the structure shows the same behaviors of the lattice parameters with pressure and chemical substitution⁶⁸. For antiferromagnetic $\text{Bi}_2\text{Sr}_2\text{CaCu}_2\text{O}_8$, the shrinking of the lattice under pressure (Fig. 4) was found in a way similar to the effect of doping^{61,62}. In fact, the reduction of the lattice parameters with the application of pressure is far beyond those found with doping^{61,62}. It is reasonable to examine whether superconductivity could be induced in $\text{Bi}_2\text{Sr}_2\text{CaCu}_2\text{O}_8$ just like other strongly correlated systems. We thus performed the magnetic susceptibility measurements on $\text{Bi}_2\text{Sr}_2\text{CaCu}_2\text{O}_8$ crystal with the same pressure environment as the Raman scattering and XRD measurements in the almost same pressure range. The results for such measurements at high pressures up to 30.2 GPa are presented in Fig. 6. The pressure was applied and measured at a temperature of about 120 K, below which the pressure was kept near constant. For each pressure, the magnetic susceptibility data were collected in the warming run. For the comparison, we show the temperature dependence of the collected signal for nearly optimally doped $\text{Bi}_2\text{Sr}_2\text{CaCu}_2\text{O}_{8+\delta}$ at ambient pressure in the inset of Fig. 6. In both experiments, the crystal was cut in the nearly same size for the measurements.

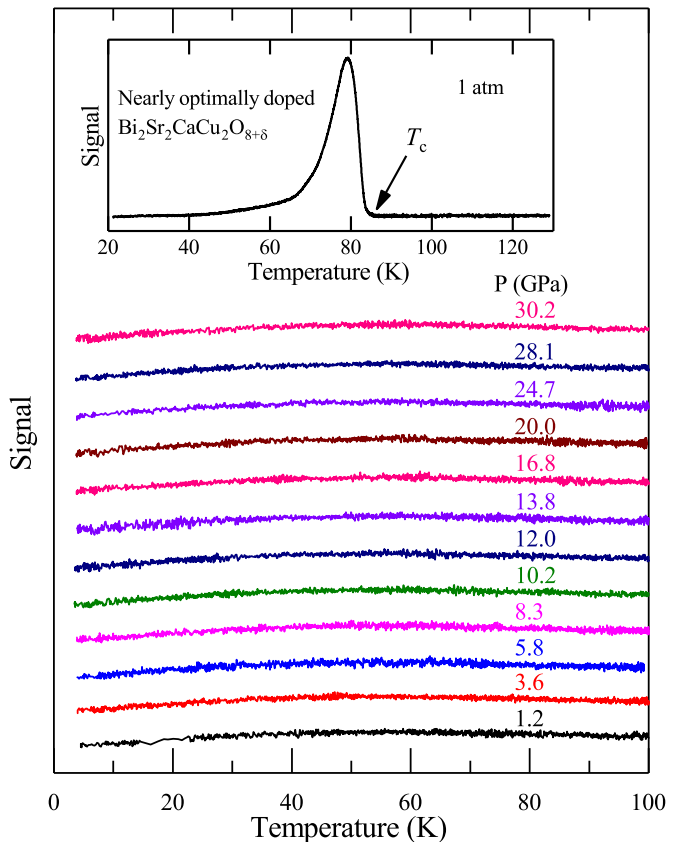


FIG. 6. Magnetic susceptibility signal versus temperature for antiferromagnetic $\text{Bi}_2\text{Sr}_2\text{CaCu}_2\text{O}_8$ single crystal at applied pressures up to 30.2 GPa. Inset: Magnetic susceptibility signal for nearly optimal doped $\text{Bi}_2\text{Sr}_2\text{CaCu}_2\text{O}_{8+\delta}$ at ambient pressure.

The magnetic susceptibility signal of nearly optimally doped $\text{Bi}_2\text{Sr}_2\text{CaCu}_2\text{O}_{8+\delta}$ exhibits a sudden jump to the peak from the flat background at temperature of 86 K followed by the gradual decline to lower temperatures (inset of Fig. 6). The starting jump point from the high-temperature side is defined as the superconducting transition due to the appearance of the Meissner effect when entering the superconducting state. Such a character for superconductivity has been observed in previous studies^{30–33,35–37} based on the developed high-pressure magnetic measurement technique²⁹.

The almost identical and featureless signals were found for $\text{Bi}_2\text{Sr}_2\text{CaCu}_2\text{O}_8$ at various pressures (Fig. 6). This behavior is substantially different from the reference signal for the nearly optimally doped $\text{Bi}_2\text{Sr}_2\text{CaCu}_2\text{O}_{8+\delta}$. The typical character for superconductivity can not be detected in the measured range of temperature and pressure. These observations demonstrate that unlike heavy fermions⁶³ or iron-based compounds⁶⁷, $\text{Bi}_2\text{Sr}_2\text{CaCu}_2\text{O}_8$ does not exhibit superconductivity by the applied pressures up to 30 GPa.

F. What parameters matter for superconductivity

The absence of superconductivity in antiferromagnetic sample upon lattice compression with pressure provides an excellent platform to test what parameters matter for superconductivity. As can be seen from Fig. 4, the application of pressure substantially shrinks the unit cell of $\text{Bi}_2\text{Sr}_2\text{CaCu}_2\text{O}_8$ compared to the effect due to doping^{61,62}. This indicates that doping alone is not enough for inducing superconductivity. To drive a system to superconduct, the pair formation is essential. For high- T_c cuprates, the decrease of J was generally observed with doping^{9,11–15,47,48}. In such a way, quasiparticles may gain the energy for pairing with the expense of J ¹⁷ if spin-mediated pairing works. The observed increase of J in $\text{Bi}_2\text{Sr}_2\text{CaCu}_2\text{O}_8$ with pressure (Fig. 3) indicates that the antiferromagnetic order does not collapse in the studied pressure range. Once the antiferromagnetism can be completely suppressed in this compound, the introduction of superconductivity is possible.

The reported nearly constant pressure derivative of T_c (dT_c/dP)⁵⁹ and universal parabolic evolution of T_c with pressure³⁵ for $\text{Bi}_2\text{Sr}_2\text{CaCu}_2\text{O}_{8+\delta}$ with different oxygen contents strongly suggest that another independent parameter controls the superconductivity besides the carrier concentration due to the chemical doping or elemental substitution. The unchanged magnetic excitations in $\text{La}_{2-x}\text{Sr}_x\text{CuO}_4$ across the entire doping regime of the phase diagram⁶⁹ indicate that T_c could be controlled by other factors rather than the magnetic excitations themselves. An inelastic neutron scattering study on $\text{La}_{2-x}\text{Sr}_x\text{CuO}_4$ revealed a strong coupling between the spin excitations and optical phonons⁷⁰. Such a coupling might be important for the formation of the charge-density wave states and superconductivity in these materials⁷¹. The quantitative spectroscopic analysis⁷² of one-dimensional antiferromagnetic cuprate chains suggested that the observed anomalously strong near-neighbor attraction probably originates from electron-phonon coupling. Indeed, without the consideration of electron-phonon interactions, it is hard to explain the observed sizable oxygen isotope effect and its evolution with adding CuO_2 plane in $\text{Bi}_2\text{Sr}_2\text{Ca}_{n-1}\text{Cu}_n\text{O}_{2n+4+\delta}$ ($n=1,2,3$)⁷³. The electronic and phononic contributions to the pairing strengths can be distinguished from the time resolution spectroscopy measurements due to their different lifetimes^{74,75}. It was found that both electronic excitations and electron-phonon interactions can not be neglected^{74,75}. For $\text{Bi}_2\text{Sr}_2\text{CaCu}_2\text{O}_{8+\delta}$, the electron-phonon coupling strength was found to behave with doping in a way similar to the T_c behavior, while the electron-spin fluctuation coupling strength decreases monotonically with doping⁷⁵. Therefore, another parameter independent of the carrier concentration is the pairing strength itself. If the strong interactions can be induced upon lattice compression with the suppression of the antiferromagnetic order, the superconductivity in $\text{Bi}_2\text{Sr}_2\text{CaCu}_2\text{O}_8$ can be expected. In this as-

pect, the observed signature of superconductivity⁷⁶ in $\text{Bi}_{1.98}\text{Sr}_{2.06}\text{Y}_{0.68}\text{CaCu}_2\text{O}_{8+\delta}$ at modest pressure of a few GPa is likely due to the interaction enhancement through the lattice modulation caused by Y substitution.

Note that the doping dependence of the electron-spin fluctuation coupling strength⁷⁵ in $\text{Bi}_2\text{Sr}_2\text{CaCu}_2\text{O}_{8+\delta}$ is similar to the evolution of J with doping^{12,13}. This similarity indicates that spin fluctuations or electronic excitations need to develop at the expense of the antiferromagnetic interactions. However, the electron-phonon coupling strength is larger than the electron-spin fluctuation coupling strength over the large doping region of the superconducting phase diagram⁷⁵. Interestingly, the electron-phonon coupling strength varies parabolically with doping⁷⁵, similar to the observed behaviors of the energy gap Δ and $2\Delta/k_B T_c$ as already reported from tunneling measurements from the underdoped regime^{77,78} to the overdoped one⁷⁹.

IV. CONCLUSIONS

In conclusion, we have conducted a comprehensive study on antiferromagnetic $\text{Bi}_2\text{Sr}_2\text{CaCu}_2\text{O}_8$ under high pressures, using Raman scattering, X-ray diffraction, and magnetic susceptibility measurements. Raman scattering measurements revealed an increase in the two-magnon frequency from approximately 3000 cm^{-1} at ambient pressure to 3550 cm^{-1} at 33.1 GPa within the applied pressure range. The lattice parameters were observed to decrease monotonically with increasing pressure without any indication for the structural transition within the studied pressure range. Under compression, the in-plane superexchange interaction J was found to increase with pressure and follow $J \sim d^{-(6.6\pm 0.2)}$ with the in-plane spacing distance at low pressures. The effects of pressure and chemical doping on the superexchange interaction and structure were discussed and compared. The implications of these parameters on superconductivity were given. Over the studied pressure range, we did not detect pressure-induced superconductivity in antiferromagnetic $\text{Bi}_2\text{Sr}_2\text{CaCu}_2\text{O}_8$. Possible factors for controlling superconductivity in high- T_c cuprates were thus drawn from the comparisons of the experiments.

V. ACKNOWLEDGEMENTS

The work at HPSTAR was supported by the National Key R&D Program of China (Grant No. 2018YFA0305900). The work at HIT was supported from the Shenzhen Science and Technology Program (Grant No. KQTD20200820113045081) and the Basic Research Program of Shenzhen (Grant No. JCYJ20200109112810241). G.D.G was supported by U.S. Department of Energy (DOE) (DE-SC0012704). V.V.S. and H.K.M. acknowledge the financial support from Shanghai Science and Technology Committee,

China (No. 22JC1410300) and Shanghai Key Laboratory of Materials Frontier Research in Extreme Environments, China (No. 22dz2260800). The XRD measurements were performed at HPCAT (Sector 16), Advanced Photon Source (APS), Argonne National Laboratory. HP-

CAT operations are supported by DOE-NNSA's Office of Experimental Sciences. The Advanced Photon Source is a U.S. DOE Office of Science User Facility operated for the DOE Office of Science by Argonne National Laboratory under Contract No. DE-AC02-06CH11357.

-
- * xjchen2@gmail.com
- 1 J. G. Bednorz and K. A. Müller, Possible high T_c superconductivity in the Ba-La-Cu-O system. *Z. Phys. B* **64**, 189 (1986).
 - 2 M. K. Wu, J. R. Ashburn, C. J. Torng, P. H. Hor, R. L. Meng, L. Gao, Z. J. Huang, Y. Q. Wang, and C. W. Chu, Superconductivity at 93 K in a new mixed-phase Y-Ba-Cu-O compound system at ambient pressure. *Phys. Rev. Lett.* **58**, 908 (1987).
 - 3 P. W. Anderson, The resonating valence bond state in La_2CuO_4 and superconductivity. *Science* **235**, 1196 (1987).
 - 4 P. W. Anderson, P. A. Lee, M. Randeria, T. M. Rice, N. Trivedi, and F. C. Zhang, The physics behind high-temperature superconducting cuprates: The 'plain vanilla' version of RVB. *J. Phys.: Condens. Matter* **16**, R755 (2004).
 - 5 P. Monthoux, A. V. Balatsky, and D. Pines, Weak-coupling theory of high-temperature superconductivity in the antiferromagnetically correlated copper oxides. *Phys. Rev. B* **46**, 14803 (1992).
 - 6 D. J. Scalapino, A common thread: The pairing interaction for unconventional superconductors. *Rev. Mod. Phys.* **84**, 1383 (2012).
 - 7 T. P. Devereaux and R. Hackl, Inelastic light scattering from correlated electrons. *Rev. Mod. Phys.* **79**, 175 (2007).
 - 8 K. B. Lyons, P. A. Fleury, J. P. Remeika, A. S. Cooper, and T. J. Negran, Dynamics of spin fluctuations in lanthanum cuprate. *Phys. Rev. B* **37**, 2353 (1988).
 - 9 S. Sugai, S. I. Shamoto, and M. Sato, Two-magnon Raman scattering in $(\text{La}_{1-x}\text{Sr}_x)_2\text{CuO}_4$. *Phys. Rev. B* **38**, 6436 (1988).
 - 10 R. R. P. Singh, P. A. Fleury, K. B. Lyons, and P. E. Sulewski, Quantitative determination of quantum fluctuations in the spin-1/2 planar antiferromagnet. *Phys. Rev. Lett.* **62**, 2736 (1989).
 - 11 K. B. Lyons, P. A. Fleury, L. F. Schneemeyer, and J. V. Waszczak, Spin fluctuations and superconductivity in $\text{Ba}_2\text{YCu}_3\text{O}_{6+\delta}$. *Phys. Rev. Lett.* **60**, 732 (1988).
 - 12 S. Sugai and T. Hosokawa, Relation between the superconducting gap energy and the two-magnon Raman peak energy in $\text{Bi}_2\text{Sr}_2\text{Ca}_{1-x}\text{Y}_x\text{Cu}_2\text{O}_{8+\delta}$. *Phys. Rev. Lett.* **85**, 1122 (2000).
 - 13 S. Sugai, H. Suzuki, Y. Takayanagi, T. Hosokawa, and N. Hayamizu, Carrier-density-dependent momentum shift of the coherent peak and the LO phonon mode in p -type high- T_c superconductors. *Phys. Rev. B* **68**, 184504 (2003).
 - 14 S. V. Zaitsev, A. A. Maksimov, and I. I. Tartakovskii, Two-magnon Raman scattering in dielectric and superconducting $\text{YBa}_2\text{Cu}_3\text{O}_{6+x}$ crystals. *J. Exp. Theor. Phys.* **111**, 582 (2010).
 - 15 Y. Li, M. Le Tacon, M. Bakr, D. Terrade, D. Manske, R. Hackl, L. Ji, M. K. Chan, N. Barišić, X. Zhao, M. Greven, and B. Keimer, Feedback effect on high-energy magnetic fluctuations in the model high-temperature superconductor $\text{HgBa}_2\text{CuO}_{4+\delta}$ observed by electronic Raman scattering. *Phys. Rev. Lett.* **108**, 227003 (2012).
 - 16 B. Mansart, J. Lorenzana, A. Mann, A. Odeh, M. Scaronigella, M. Chergui, and F. Carbone, Coupling of a high-energy excitation to superconducting quasiparticles in a cuprate from coherent charge fluctuation spectroscopy. *Proc. Natl. Acad. Sci. U.S.A.* **110**, 4539 (2012).
 - 17 N. Lin, E. Gull, and A. J. Millis, Two-particle response in cluster dynamical mean-field theory: Formalism and application to the Raman response of high-temperature superconductors. *Phys. Rev. Lett.* **109**, 106401 (2012).
 - 18 L. C. Wang, G. H. He, Z. C. Yang, M. Garcia-Fernandez, A. Nag, K. J. Zhou, M. Minola, M. Le Tacon, B. Keimer, Y. Y. Peng, and Y. Li, Paramagnons and high-temperature superconductivity in a model family of cuprates. *Nat. Commun.* **575**, 156 (2022).
 - 19 S. L. Cooper, G. A. Thomas, A. J. Millis, P. E. Sulewski, J. Orenstein, D. H. Rapkine, S. W. Cheong, and P. L. Trevor, Optical studies of gap, exchange, and hopping energies in the insulating cuprates. *Phys. Rev. B* **42**, 10785 (1990).
 - 20 H. K. Mao, X. J. Chen, Y. Ding, B. Li, and L. Wang, Solids, liquids, and gases under high pressure. *Rev. Mod. Phys.* **90**, 015007 (2018).
 - 21 A. F. Goncharov and V. V. Struzhkin, Raman spectroscopy of metals, high-temperature superconductors and related materials under high pressure. *Journal of Raman Spectroscopy* **34**, 532 (2003).
 - 22 M. C. Aronson, S. B. Dierker, B. S. Dennis, S. W. Cheong, and Z. Fisk, Pressure dependence of the superexchange interaction in antiferromagnetic La_2CuO_4 . *Phys. Rev. B* **44**, 4657 (1991).
 - 23 M. I. Erements, A. V. Lomsadze, V. V. Struzhkin, A. A. Maksimov, A. V. Puchkov, and I. I. Tartakovskii, Effect of high hydrostatic pressure on the exchange interaction in Eu_2CuO_4 single crystals. *Pis'ma Zh. Eksp. Teor. Fiz.* **54**, 376 (1991) [*JETP Lett.* **54**, 372 (1991)].
 - 24 V. V. Struzhkin, A. F. Goncharov, H. K. Mao, R. J. Hemley, S. W. Moore, J. M. Graybeal, J. Sarrao, and Z. Fisk, Coupled magnon-phonon excitations in $\text{Sr}_2\text{CuCu}_2\text{O}_2$ at high pressure. *Phys. Rev. B* **62**, 3895 (2000).
 - 25 A. Maksimov and I. Tartakovskii, Electronic and two-magnon light scattering in oxide superconducting crystals. *J. Supercond.* **7**, 439 (1994).
 - 26 T. Cuk, V. V. Struzhkin, T. P. Devereaux, A. F. Goncharov, C. A. Kendziora, H. Eisaki, H. K. Mao, and Z. X. Shen, Uncovering a pressure-tuned electronic transition in $\text{Bi}_{1.98}\text{Sr}_{2.06}\text{Y}_{0.68}\text{Cu}_2\text{O}_{8+\delta}$ using Raman scattering and X-ray diffraction. *Phys. Rev. Lett.* **100**, 217003 (2008).
 - 27 M. Kakihana, M. Osada, M. Käll, L. Börjesson, H. Mazaki, H. Yasuoka, M. Yashima, and M. Yoshimura, Raman-active phonons in $\text{Bi}_2\text{Sr}_2\text{Ca}_{1-x}\text{Y}_x\text{Cu}_2\text{O}_{8+d}$ ($x=0-1$): Effects of hole filling and internal pressure induced by Y doping for Ca, and implications for phonon assignments. *Phys. Rev. B* **53**, 11796 (1996).

- ²⁸ G. D. Gu, K. Takamuku, N. Koshizuka, and S. Tanaka, Large single crystal Bi-2212 along the c -axis prepared by floating zone method. *J. Cryst. Growth* **130**, 325 (1993).
- ²⁹ Y. A. Timofeev, V. V. Struzhkin, R. J. Hemley, H. K. Mao, and E. A. Gregoryanz, Improved techniques for measurement of superconductivity in diamond anvil cells by magnetic susceptibility. *Rev. Sci. Instrum.* **73**, 371 (2002).
- ³⁰ X. J. Chen, V. V. Struzhkin, Y. Yu, A. F. Goncharov, C. T. Lin, H. K. Mao, and R. J. Hemley, Enhancement of superconductivity by pressure-driven competition in electronic order. *Nature* **466**, 950 (2010).
- ³¹ V. V. Struzhkin, R. J. Hemley, H. K. Mao, and Y. A. Timofeev, Superconductivity at 10–17 K in compressed sulphur. *Nature* **390**, 382 (1997).
- ³² V. V. Struzhkin, M. I. Erements, W. Gan, H. K. Mao, and R. J. Hemley, Superconductivity in dense lithium. *Science* **298**, 1213 (2002).
- ³³ X. J. Chen, V. V. Struzhkin, Z. G. Wu, R. E. Cohen, S. Kung, H. K. Mao, R. J. Hemley, and A. N. Christensen, Electronic stiffness of a superconducting niobium nitride single crystal under pressure. *Phys. Rev. B* **72**, 094514 (2005).
- ³⁴ X. J. Chen, V. V. Struzhkin, Z. G. Wu, H. Q. Lin, R. J. Hemley, and H. K. Mao, Unified picture of the oxygen isotope effect in cuprate superconductors. *Proc. Natl. Acad. Sci. U.S.A.* **104**, 3732 (2007).
- ³⁵ X. J. Chen, V. V. Struzhkin, R. J. Hemley, H. K. Mao, and C. Kendziora, High-pressure phase diagram of $\text{Bi}_2\text{Sr}_2\text{CaCu}_2\text{O}_{8+\delta}$ single crystals. *Phys. Rev. B* **70**, 214502 (2004).
- ³⁶ J. B. Zhang, V. V. Struzhkin, W. G. Yang, H. K. Mao, H. Q. Lin, Y. C. Ma, N. L. Wang, and X. J. Chen, Effects of pressure and distortion on superconductivity in $\text{Tl}_2\text{Ba}_2\text{CaCu}_2\text{O}_{8+\delta}$. *J. Phys.: Condens. Matter* **27**, 445701 (2015).
- ³⁷ S. B. Wang, J. B. Zhang, J. Y. Yan, X. J. Chen, V. Struzhkin, W. Tabis, N. Barišić, M. K. Chan, C. Dorow, X. D. Zhao, M. Greven, W. L. Mao, and T. Geballe, Strain derivatives of T_c in $\text{HgBa}_2\text{CuO}_{4+\delta}$: The CuO_2 plane alone is not enough. *Phys. Rev. B* **89**, 024515 (2014).
- ³⁸ H. K. Mao, J. A. Xu, and P. M. Bell, Calibration of the ruby pressure gauge to 800 kbar under quasi-hydrostatic conditions. *J. Geophys. Res.* **91**, 4673 (1986).
- ³⁹ A. P. Hammersley, S. O. Svensson, M. Hanfland, A. N. Fitch, and D. Hausermann, Two-dimensional detector software: From real detector to idealised image or two-theta scan. *High Pressure Res.* **14**, 235 (1996).
- ⁴⁰ B. H. Toby and R. B. Von Dreele, GSAS-II: The genesis of a modern open-source all purpose crystallography software package. *J. Appl. Crystallogr.* **46**, 544 (2013).
- ⁴¹ N. Fukushima, H. Niu, and K. Ando, Electrical and magnetic properties in $\text{Bi}_2\text{Sr}_2\text{Ca}_{1-x}\text{Y}_x\text{Cu}_2\text{O}_{8+\delta}$. *Jpn. J. Appl. Phys.* **27**, L1432 (1988).
- ⁴² B. I. Belevtsev, N. V. Dalakova, A. S. Panfilov, and E. Y. Beliayev, Anomalies of conductivity behavior near the paramagnetic antiferromagnetic transition in single-crystals $\text{La}_2\text{CuO}_{4+\delta}$. *Physica B* **405**, 1307 (2010).
- ⁴³ A. Maeda, M. Hase, I. Tsukada, K. Noda, S. Takebayashi, and K. Uchinokura, Physical properties of $\text{Bi}_2\text{Sr}_2\text{Ca}_{n-1}\text{Cu}_n\text{O}_y$ ($n=1,2,3$). *Phys. Rev. B* **41**, 6418 (1990).
- ⁴⁴ W. H. Weber and G. W. Ford, Simple model for the linewidth of the two-magnon Raman feature observed in high- T_c superconductors. *Phys. Rev. B* **40**, 6890 (1989).
- ⁴⁵ H. L. Liu, G. Blumberg, M. V. Klein, P. Guptasarma, and D. G. Hinks, c -axis electronic Raman scattering in $\text{Bi}_2\text{Sr}_2\text{CaCu}_2\text{O}_{8+\delta}$. *Phys. Rev. Lett.* **82**, 3524 (1999).
- ⁴⁶ N. N. Kovaleva, A. V. Boris, T. Holden, C. Ulrich, B. Liang, C. T. Lin, B. Keimer, C. Bernhard, J. L. Tallon, D. Munzar, and A. M. Stoneham, c -axis lattice dynamics in Bi-based cuprate superconductors. *Phys. Rev. B* **69**, 054511 (2004).
- ⁴⁷ G. Blumberg, R. Liu, M. V. Klein, W. C. Lee, D. M. Ginsberg, C. Gu, B. W. Veal, and B. Dabrowski, Two-magnon Raman scattering in cuprate superconductors: Evolution of magnetic fluctuations with doping. *Phys. Rev. B* **49**, 13295 (1994).
- ⁴⁸ M. Rübhausen, C. T. Rieck, N. Dieckmann, K. O. Subke, A. Bock, and U. Merkt, Inelastic light scattering at high-energy excitations in doped cuprate superconductors. *Phys. Rev. B* **56**, 14797 (1997).
- ⁴⁹ Y. Gao, P. Coppens, D. E. Cox, and A. R. Moodenbaugh, Combined X-ray single-crystal and neutron powder refinement of modulated structures and application to the incommensurately modulated structure of $\text{Bi}_2\text{Sr}_2\text{Ca}_{1-x}\text{Y}_x\text{Cu}_2\text{O}_{8+y}$. *Acta Crystallogr. A* **49**, 141 (1993).
- ⁵⁰ J. S. Olsen, S. Steenstrup, L. Gerward, and B. Sundqvist, High pressure studies up to 50 GPa of Bi-based high- T_c superconductors. *Phys. Scr.* **44**, 211 (1991).
- ⁵¹ J. B. Zhang, L. Y. Tang, J. Zhang, Z. X. Qin, X. J. Zeng, J. Liu, J. S. Wen, Z. J. Xu, G. D. Gu, and X. J. Chen, Pressure-induced isostructural phase transition in $\text{Bi}_2\text{Sr}_2\text{CaCu}_2\text{O}_{8+\delta}$. *Chin. Phys. C* **37**, 088003 (2013).
- ⁵² S. A. Sunshine, T. Siegrist, L. F. Schneemeyer, D. W. Murphy, R. J. Cava, B. Batlogg, R. B. van Dover, R. M. Fleming, S. H. Glarum, S. Nakahara, R. Farrow, J. J. Krajewski, S. M. Zahurak, J. V. Waszczak, J. H. Marshall, P. Marsh, L. W. Rupp, and W. F. Peck, Structure and physical properties of single crystals of the 84-K superconductor $\text{Bi}_{2.2}\text{Sr}_2\text{Ca}_{0.8}\text{Cu}_2\text{O}_{8+\delta}$. *Phys. Rev. B* **38**, 893 (1988).
- ⁵³ Y. Gao, P. Lee, P. Coppens, M. A. Subramanian, and A. W. Sleight, The incommensurate modulation of the 2212 Bi-Sr-Ca-Cu-O superconductor. *Science* **241**, 954 (1988).
- ⁵⁴ V. Petricek, Y. Gao, P. Lee, and P. Coppens, X-ray analysis of the incommensurate modulation in the 2:2:1:2 Bi-Sr-Ca-Cu-O superconductor including the oxygen atoms. *Phys. Rev. B* **42**, 387 (1990).
- ⁵⁵ P. A. Miles, S. J. Kennedy, G. J. McIntyre, G. D. Gu, G. S. Russell, and N. Koshizuka, Refinement of the incommensurate structure of high quality Bi-2212 single crystals from a neutron diffraction study. *Physica C* **294**, 275 (1998).
- ⁵⁶ F. Birch, Finite elastic strain of cubic crystals. *Phys. Rev.* **71**, 809 (1947).
- ⁵⁷ Y. Tajima, M. Hikita, M. Suzuki, and Y. Hidaka, Pressure-effect study on high- T_c superconducting single crystal of 84 K Bi-Sr-Ca-Cu-O system. *Physica C* **158**, 237 (1989).
- ⁵⁸ J. D. Yu, S. Sasaki, H. Sugiura, T. Huang, Y. Inaguma, and M. Itoh, Compressibility and pressure dependence of charge transfer and T_c in pristine and iodine-intercalated single crystals of $\text{Bi}_{2.2}\text{Sr}_{1.8}\text{CaCu}_2\text{O}_{8+\delta}$. *Physica C* **281**, 45 (1997).
- ⁵⁹ R. Sieburger, P. Müller, and J. S. Schilling, Pressure dependence of the superconducting transition temperature in $\text{Bi}_2\text{Sr}_2\text{CaCu}_2\text{O}_{8+y}$ as a function of oxygen content. *Physica C* **181**, 335 (1991).
- ⁶⁰ I. K. Drozdov, I. Pletikosić, C. K. Kim, K. Fujita, G. D. Gu, J. C. Séamus Davis, P. D. Johnson, I. Božović, and T.

- Valla, Phase diagram of $\text{Bi}_2\text{Sr}_2\text{CaCu}_2\text{O}_{8+\delta}$ revisited. *Nat. Commun.* **9**, 5210 (2018).
- ⁶¹ W. A. Groen and D. M. de Leeuw, Oxygen content, lattice constants and T_c of $\text{Bi}_2\text{Sr}_2\text{CaCu}_2\text{O}_{8+\delta}$. *Physica C* **159**, 417 (1989).
- ⁶² B. Liang, C. T. Lin, A. Maljuk, and Y. Yan, Effect of vacuum annealing on the structure and superconductivity of $\text{Bi}_2\text{Sr}_2\text{CaCu}_2\text{O}_{8+\delta}$ single crystals. *Physica C* **366**, 254 (2002).
- ⁶³ N. D. Mathur, F. M. Grosche, S. R. Julian, I. R. Walker, D. M. Freye, R. K. W. Haselwimmer, and G. G. Lonzarich, Magnetically mediated superconductivity in heavy fermion compounds. *Nature* **394**, 39 (1998).
- ⁶⁴ T. Park, F. Ronning, H. Q. Yuan, M. B. Salamon, R. Movshovich, J. L. Sarrao, and J. D. Thompson, Hidden magnetism and quantum criticality in the heavy fermion superconductor CeRhIn_5 . *Nature* **440**, 65 (2006).
- ⁶⁵ P. S. Normile, S. Heathman, M. Idiri, P. Boulet, J. Rebizant, F. Wastin, G. H. Lander, T. Le Bihan, and A. Lindbaum, High-pressure structural parameters of the superconductors CeMIn_5 and PuMGa_5 ($M=\text{Co,Rh}$). *Phys. Rev. B* **72**, 184508 (2005).
- ⁶⁶ M. Rotter, M. Tegel, and D. Johrendt, Superconductivity at 38 K in the iron arsenide $\text{Ba}_{1-x}\text{K}_x\text{Fe}_2\text{As}_2$. *Phys. Rev. Lett.* **101**, 107006 (2008).
- ⁶⁷ P. L. Alireza, Y. T. Chris Ko, J. Gillett, C. M. Petrone, J. M. Cole, G. G. Lonzarich, and S. E. Sebastian, Superconductivity up to 29 K in SrFe_2As_2 and BaFe_2As_2 at high pressures. *J. Phys.: Condens. Matter* **21**, 012208 (2008).
- ⁶⁸ S. A. J. Kimber, A. Kreyssig, Y. Z. Zhang, H. O. Jeschke, R. Valenti, F. Yokaichiya, E. Colombier, J. Q. Yan, T. C. Hansen, T. Chatterji, R. J. McQueeney, P. C. Canfield, A. I. Goldman, and D. N. Argyriou, Similarities between structural distortions under pressure and chemical doping in superconducting BaFe_2As_2 . *Nat. Mater.* **8**, 471 (2009).
- ⁶⁹ M. P. M. Dean, G. Dellea, R. S. Springell, F. Yakhov-Harris, K. Kummer, N. B. Brookes, X. Liu, Y. J. Sun, J. Strle, T. Schmitt, L. Braicovich, G. Ghiringhelli, I. Božović, and J. P. Hill, Persistence of magnetic excitations in $\text{La}_{2-x}\text{Sr}_x\text{CuO}_4$ from the undoped insulator to the heavily overdoped non-superconducting metal. *Nat. Mater.* **12**, 1019 (2013).
- ⁷⁰ K. Ikeuchi, S. Wakimoto, M. Fujita, T. Fukuda, R. Kajimoto, and M. Arai, Spin excitations coupled with lattice and charge dynamics in $\text{La}_{2-x}\text{Sr}_x\text{CuO}_4$. *Phys. Rev. B* **105**, 014508 (2022).
- ⁷¹ V. V. Struzhkin and X. J. Chen, Magnon-phonon coupling and implications for charge-density wave states and superconductivity in cuprates. *Low Temp. Phys.* **42**, 884 (2016).
- ⁷² Z. Y. Chen, Y. Wang, S. N. Rebec, T. Jia, M. Hashimoto, D. H. Lu, B. Moritz, R. G. Moore, T. P. Devereaux, and Z. X. Shen, Anomalously strong near-neighbor attraction in doped 1D cuprate chains. *Science* **373**, 1235 (2021).
- ⁷³ X. J. Chen, B. Liang, C. Ulrich, C. T. Lin, V. V. Struzhkin, Z. G. Wu, R. J. Hemley, H. K. Mao, and H. Q. Lin, Oxygen isotope effect in $\text{Bi}_2\text{Sr}_2\text{Ca}_{n-1}\text{Cu}_n\text{O}_{2n+4+\delta}$ ($n=1,2,3$) single crystals. *Phys. Rev. B* **76**, 140502(R) (2007).
- ⁷⁴ S. Dal Conte, C. Giannetti, G. Coslovich, F. Cilento, D. Bossini, T. Abebaw, F. Banfi, G. Ferrini, H. Eisaki, M. Greven, A. Damascelli, D. van der Marel, and F. Parmigiani, Disentangling the electronic and phononic glue in a high- T_c superconductor. *Science* **335**, 1600 (2012).
- ⁷⁵ E. E. M. Chia, D. Springer, S. K. Nair, X. Q. Zou, S. A. Cheong, C. Panagopoulos, T. Tamegai, H. Eisaki, S. Ishida, S. Uchida, A. J. Taylor, and J. X. Zhu, Doping dependence of the electron-phonon and electron-spin fluctuation interactions in the high- T_c superconductor $\text{Bi}_2\text{Sr}_2\text{CaCu}_2\text{O}_{8+\delta}$. *New J. Phys.* **15**, 103027 (2013).
- ⁷⁶ T. Cuk, D. A. Zocco, H. Eisaki, V. Struzhkin, F. M. Grosche, M. B. Maple, and Z. X. Shen, Signatures of pressure-induced superconductivity in insulating $\text{Bi}_{1.98}\text{Sr}_{2.06}\text{Y}_{0.68}\text{CaCu}_2\text{O}_{8+\delta}$. *Phys. Rev. B* **81**, 184509 (2010).
- ⁷⁷ N. Miyakawa, P. Guptasarma, J. F. Zasadzinski, D. G. Hinks, and K. E. Gray, Strong Dependence of the Superconducting Gap on Oxygen Doping from Tunneling Measurements on $\text{Bi}_2\text{Sr}_2\text{CaCu}_2\text{O}_{8-\delta}$. *Phys. Rev. Lett.* **80**, 157 (1998).
- ⁷⁸ N. Miyakawa, J. F. Zasadzinski, L. Ozyuzer, P. Guptasarma, D. G. Hinks, C. Kendziora, and K. E. Gray, Predominantly Superconducting Origin of Large Energy Gaps in Underdoped $\text{Bi}_2\text{Sr}_2\text{CaCu}_2\text{O}_{8+\delta}$ from Tunneling Spectroscopy. *Phys. Rev. Lett.* **83**, 1018 (1999).
- ⁷⁹ Y. DeWilde, N. Miyakawa, P. Guptasarma, M. Iavarone, L. Ozyuzer, J. F. Zasadzinski, P. Romano, D. G. Hinks, C. Kendziora, G. W. Crabtree, and K. E. Gray, Unusual Strong-Coupling Effects in the Tunneling Spectroscopy of Optimally Doped and Overdoped $\text{Bi}_2\text{Sr}_2\text{CaCu}_2\text{O}_{8+\delta}$. *Phys. Rev. Lett.* **80**, 153 (1998); Erratum: *Phys. Rev. Lett.* **81**, 492 (1998).